Supporting Information for

Targeted Fluorescence Enhancement of Acridones by Hydrogen Bonding in Solution and Solid State

Matthias Jantz[1], David Klaverkamp[1], Benedikt Bendel[2], Takin Haj Hassani Sohi[3], Martin H. Polko[3], Lennart Bunnemann[4], Tobias Böhmer[5], Markus Putscher[5], Christel M. Marian[5], Constantin Czekelius[4]*, Vera Vasylyeva[3]*, Markus Suta[2], and Peter Gilch[1]*

[1]Institut für Physikalische Chemie, Mathematisch-Naturwissenschaftliche Fakultät, Heinrich-Heine-Universität Düsseldorf, Universitätsstr. 1, 40225 Düsseldorf, Germany

[2]Anorganische Photoaktive Materialien, Institut für Anorganische Chemie und Strukturchemie, Mathematisch-Naturwissenschaftliche Fakultät, Heinrich-Heine-Universität Düsseldorf, Universitätsstr. 1, 40225 Düsseldorf, Germany

[3]Molecular Crystal Engineering, Institut für Anorganische Chemie und Strukturchemie, Mathematisch-Naturwissenschaftliche Fakultät, Heinrich-Heine-Universität Düsseldorf, Universitätsstr. 1, 40225 Düsseldorf, Germany

[4]Institut für Organische Chemie und Makromolekulare Chemie, Mathematisch-Naturwissenschaftliche Fakultät, Heinrich-Heine-Universität Düsseldorf, Universitätsstr. 1, 40225 Düsseldorf, Germany

[5]Institut für Theoretische Chemie und Computerchemie, Mathematisch-Naturwissenschaftliche Fakultät, Heinrich-Heine-Universität Düsseldorf, Universitätsstr. 1, 40225 Düsseldorf, Germany

*Corresponding authors' e-mails: constantin.czekelius@hhu.de, vera.vasylyeva-shor@hhu.de and gilch@hhu.de

Details of data evaluation and modelling

The analysis of the titration curve in Figure 2 relied on a 1:1 binding model $NMA+SCat \rightleftharpoons NMA\cdots SCat$ in which NMA and SCat form a hydrogen-bonded complex $NMA\cdots SCat$. Considering the law of mass action, the dissociation constant (K_D) of NMA···SCat depends on the equilibrium concentrations of NMA, SCat and the coordinated form NMA···SCat,

$$K_D = \frac{[NMA][SCat]}{[NMA\cdots SCat]}. \quad \text{(S1)}$$

It should be noted that K_D is an effective value, as SCat molecules presumably forms hydrogen bonds among each other. For the coordination of NMA and SCat, the hydrogen bond between the SCat molecules must first be disrupted. Since SCat is present in excess, it can be expected that $[SCat]$ corresponds approximately to the initial concentration $[SCat]_0$,

$$[SCat] \approx [SCat]_0. \quad \text{(S2)}$$

The ratio between the free and coordinated form can be calculated accordingly as follows,

$$\frac{[NMA]}{[NMA\cdots SCat]} = \frac{K_D}{[SCat]_0}. \quad \text{(S3)}$$

To determine the K_D value, the change in fluorescence signal Δy of NMA upon SCat addition was recorded as a function of the concentration $[SCat]_0$. The following relation between the signal change Δy and the concentration $[SCat]_0$ can be derived:[1,2]

$$\triangle y = \frac{y_m - y_0}{2[NMA]_0} \cdot \left([NMA]_0 + [SCat]_0 + K_D - \sqrt{([NMA]_0 + [SCat]_0 + K_D)^2 - 4 \cdot [NMA]_0 \cdot [SCat]_0}\right). \quad \text{(S4)}$$

y_m is the fluorescence signal at infinite SCat concentration and y_0 is the fluorescence signal in the absence of SCat. Fitting the experimental data to this function affords the equilibrium constant K_D and the fluorescence signal for infinite $[SCat]$.

The dissociation constant K_D can be related with a standard Gibbs free energy ΔG_D^0 consisting of an enthalpic (ΔH_D^0) and entropic (ΔS_D^0) contribution,

$$\frac{K_D}{c_0} = e^{-\frac{\Delta G_D^0}{RT}} = e^{-\frac{\Delta H_D^0}{RT}} \cdot e^{+\frac{\Delta S_D^0}{R}}. \quad \text{(S5)}$$

Here, c_0 = 1 mol/l is the reference concentration. Assuming that the complexation by SCat does not change the vibrational degrees of freedom, the reaction entropy ΔS_D^0 can be related with the molar volume $\overline{V}_{NMA\cdots SCat}$ of the contact pair and the reference concentration,[3, 4]

$$\Delta S_D^0 = R \cdot ln\left(\frac{1}{c_0 \cdot \overline{V}_{NMA\cdots SCat}}\right). \quad \text{(S6)}$$

$\overline{V}_{NMA\cdots SCat}$ was obtained by multiplying the van der Waals volume of the contact pair (522.736 Å^3), with Avogadro´s number N_a, $\overline{V}_{NMA\cdots SCat}$ = 0.315 l/mol, The van der Waals volume was computed using the MoloVol software[5] with the quantum-chemically optimized structure as an input. Combining eq. S5 and S6 relates the dissociation constant K_D with the reaction enthalpy ΔH_D^0,

$$\Delta H_D^0 = RT \cdot ln(K_D \cdot \overline{V}_{NMA\cdots SCat}). \quad \text{(S7)}$$

Note that for the dissociation the enthalpy $\Delta H_D^0 > 0$ and the entropy $\Delta S_D^0 > 0$.

The fluorescence quantum yield (ϕ_{fl}) is the product of the radiative rate constant (k_{rad}) and the lifetime (τ),

$$\phi_{fl} = k_{rad} \cdot \tau. \quad \text{(S8)}$$

If the constant k_{rad} is not affected by complexation, the relative increase of the fluorescence quantum yield must be proportional to the increase of the relative, averaged lifetime.

However, as the fluorescence spectrum of NMA⋯SCat is shifted with respect to the one of free NMA, a correction factor X to account for the different coverage of the emission spectra by the detection bandpass must be introduced,

$$X = \frac{\frac{Area_{Bandpass}^{NMA}}{Area_{Total}^{NMA}}}{\frac{Area_{Bandpass}^{NMA\cdots SCat}}{Area_{Total}^{NMA\cdots SCat}}}. \quad \text{(S9)}$$

Here, $Area_{Bandpass}^{NMA}$ is the spectral integral of the NMA fluorescence for the interval given by the detection bandpass in the TCSPC experiment. $Area_{Total}^{NMA}$ is the spectral integral covering the NMA fluorescence completely. $Area_{Bandpass}^{NMA\cdots SCat}$ and $Area_{Total}^{NMA\cdots SCat}$ are respective values for complexed NMA. This correction factor takes into account that for a set spectral detection window varying portion of the fluorescence spectra of the species fall into this window (Figure S1).

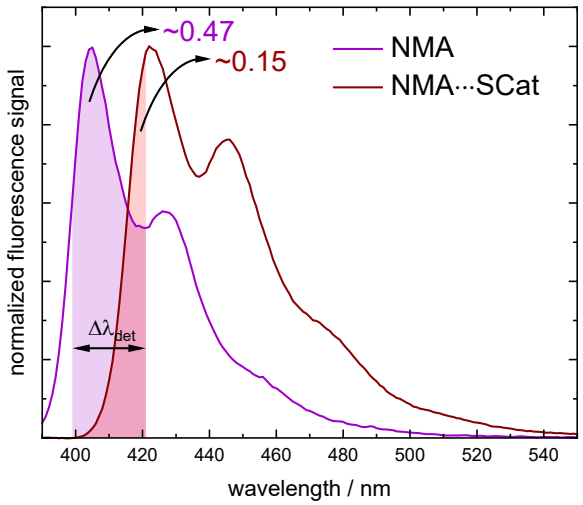

Figure S1: Normalized emission spectra of NMA (9.3 µM) in the absence (purple) and presence of SCat (2.2 mM, dark red). The residual contribution of free NMA was scaled and subtracted to obtain the NMA · · · SCat spectrum. The relative portion of the integrals which are covered by the detection bandpass ($\Delta\lambda_{det}$) centered at 410 nm are highlighted with their respective color.

X results from the ratio from the integral covered by the bandpass of each species to the respective integral over the whole emission region. The corrected, averaged lifetime $\overline{\tau^{cor}}$ for the respective concentration can be calculated as follows:

$$\overline{\tau^{cor}}([SCat]) = \frac{\sum_{i=1,2,4} A_{NMA,i}([SCat]) \cdot \tau_{NMA,i} + X \cdot A_{NMA\cdots SCat,3}([SCat]) \cdot \tau_{NMA\cdots SCat,3}}{\sum_{i=1,2,4} A_{NMA,i}([SCat]) + X \cdot A_{NMA\cdots SCat,3}([SCat])}. \quad \text{(S10)}$$

83

84 The relative, corrected, averaged lifetime is obtained by dividing $\overline{\tau^{cor}}([SCat])$ by $\overline{\tau^{cor}}([0])$. The
85 amplitudes and lifetimes obtained from the fits to the TCSPC data are shown in Table S1 while
86 the corrected amplitudes and lifetimes are shown in Table S2.

Femtosecond Transient Absorption Spectroscopy of NMA and NMA···SCat in Solution

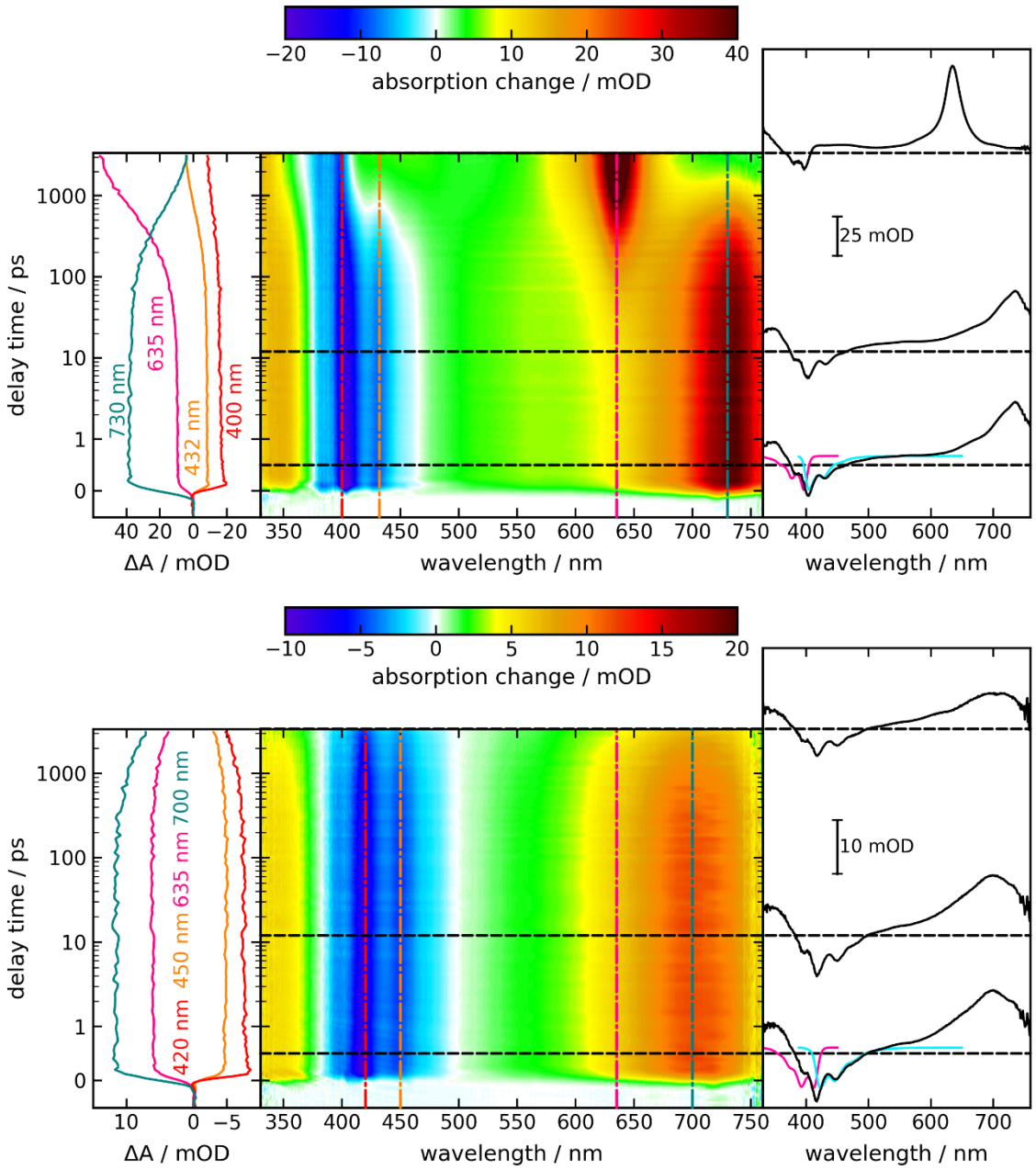

Figure S2: Femtosecond transient absorption (fsTA) measurements on NMA (top; 1.86 mM (NMA)) and NMA in the presence of SCat (bottom; 1.5 mM (SCat)) in toluene. The excitation wavelength was set to 400 nm. In the central contour plots, the difference absorption signal is color-coded. Vertical lines mark the spectral positions corresponding to the time traces displayed on the left, while horizontal lines indicate selected delay times for the difference spectra shown on the right. The spectra at 0.6 ps (black) where compared to the normalized ground state absorption spectra (pink) and fluorescence (light blue) converted into stimulated emission spectra.[6, 7] The plot for NMA···SCat was corrected for the minor contribution of free NMA.

The determination of the triplet quantum yield (ϕ_T) is based on the comparison of the ground state bleach (GSB) signal at early and late delay times. After 3.3 ns no signal contribution from the stimulated emission is left. The remaining GSB signal can thus be attributed to molecules in the triplet state. To obtain the yield ϕ_T, the absorption spectrum of NMA was flipped, scaled and aligned with the respective ground state bleach at 200 fs and 3.3 ns after excitation (Figure S3). The fraction of the scaling factors for early and late delay times yields ϕ_T to be ~0.9.

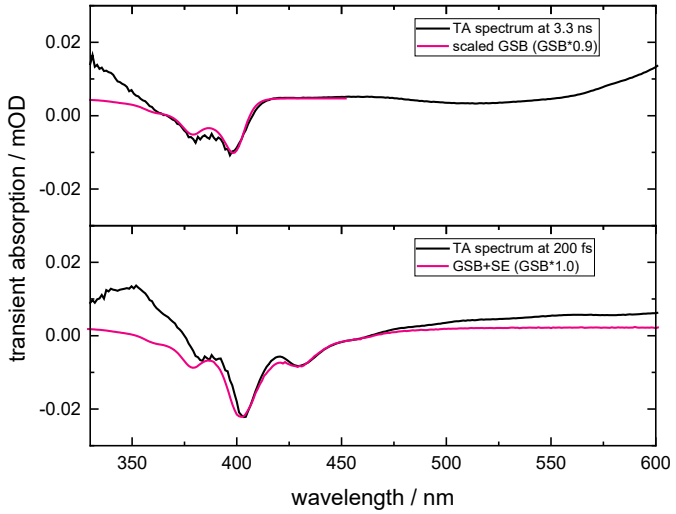

Figure S3: Determination of the triplet yield ϕ_T of NMA in toluene. In the lower panel the transient absorption spectrum at 200 fs is shown in black while the sum of the flipped absorption and stimulated emission spectra is shown in pink (scaling factor 1.0). In the upper panel the transient absorption spectrum at 3.3 ns is shown in black, while the flipped absorption spectrum is shown in pink (scaling factor 0.9).

The determination of the equilibrium constant *K* between the $^1\pi\pi^*$ and $^3n\pi^*$ states is detailed in ref.[8] and relies on a single-exponential fit of the spectrally integrated stimulated emission. The fit yields the value of the integral at time zero (I_0) and after equilibration (I_{eq})(Figure S4). These values are related with the equilibrium constant *K via*,

$$\frac{I_0 - I_{eq}}{I_{eq}} = K = \frac{[\,^3n\pi^*]}{[\,^1\pi\pi^*]}. \qquad \text{(S11)}$$

Note, that K is hereby defined with $^3n\pi^*$ as the product. The fit yields a K value of 0.63 and a time constant of 56 ps. Assuming, that only one triplet sub-level is populated and entropy changes can be neglected, the constant K can be correlated to a single-triplet energy gap (ΔE_{ST}) as follows,

$$\Delta E_{ST} = -k_B T \cdot lnK. \quad \text{(S12)}$$

With the thermal energy $k_B T$ at room temperature, the $^3n\pi^*$ state is placed 0.012 eV (95 cm^{-1}) above the $^1\pi\pi^*$ one. For the NMA···SCat complex no indications for an equilibration are found.

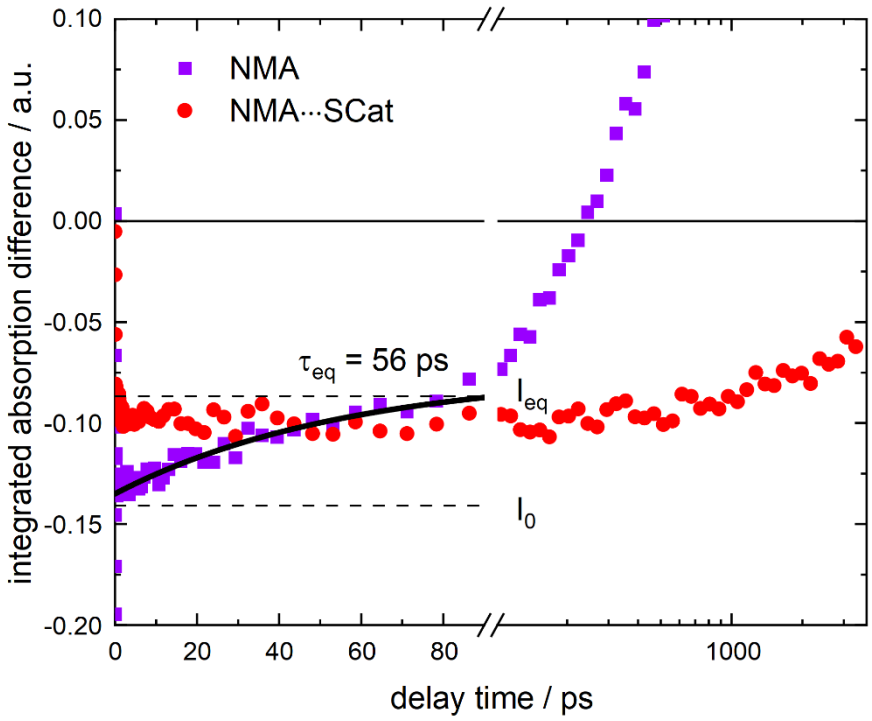

Figure S4: Decay of the spectrally integrated stimulated emission (SE) of NMA (red) and NMA+SCat (purple) in toluene. The boundaries of integration were set within the SE, where SE and the ground state bleach do not overlap (NMA: 420-500 nm, NMA···SCat: 440-550 nm). For NMA the increase in the integrated absorption difference is fitted single-exponentially at early delay times and the parameters I_0 and I_{eq} are marked with dashed lines.

Amplitudes and Time Constants of the TCSPC Measurement in Solution

Table S1: Amplitudes (A) and time constants (τ) obtained from the fits to the TCSPC data of NMA in toluene in the absence and in the presence of different SCat concentrations. Depicted are also the amplitude-weighted average lifetimes ($\overline{\tau}$) and the increase of the averaged lifetime ($\overline{\tau_{rel}}$) compared to the lifetime of NMA in absence of SCat.

[SCat] / 10^{-4} M	A_1	τ_1 / ns	A_2	τ_2 / ns	A_3	τ_3 / ns	A_4	τ_4 / ns	$\overline{\tau}$ / ns	$\overline{\tau_{rel}}$
0	0.5959± 0.0358	0.7134± 0.0214	0.4040± 0.0566	1.0922± 0.0218			0.0001± 0.00001	18.2915 ±0.0915	0.8686± 0.0686	1.0000
1.84	0.4487± 0.1436	0.6917± 0.0692	0.3725± 0.1674	1.1030± 0.0993	0.1787± 0.0054	6.8600± 0.0343	0.0001± 0.00001	60.7553 ±0.3038	1.9550± 0.2184	2.2521
3.69	0.5482± 0.0384	0.7510± 0.0451	0.1541± 0.0986	1.3545± 0.2167	0.2975± 0.0238	6.8696± 0.0343	0.0001± 0.00002	59.8018 ±0.2990	2.6733± 0.2173	3.0794
5.53	0.4704± 0.0517	0.7340± 0.0514	0.1517± 0.0971	1.3473± 0.2290	0.3777± 0.0264	6.8682± 0.0343	0.0002± 0.00002	57.4952 ±0.2875	3.1581± 0.2311	3.6379
6.33	0.4516± 0.0587	0.7437± 0.0595	0.1366± 0.0984	1.3649± 0.2730	0.4117± 0.0288	6.8762± 0.0344	0.0002± 0.00002	62.2727 ±0.3114	3.3702± 0.2480	3.8822
7.38	0.4565± 0.0365	0.7591± 0.0455	0.0973± 0.0613	1.5299± 0.0321	0.4461± 0.0223	6.8777± 0.0344	0.0002± 0.00002	58.0402 ±0.2902	3.5746± 0.1838	4.1177
22.1	0.3352± 0.0101	0.7919± 0.0238	0.0449± 0.0081	2.9059± 0.6102	0.6196± 0.0062	6.9126± 0.0346	0.0003± 0.00002	59.7140 ±0.2986	4.6970± 0.0611	5.4106
22.1 (412 nm)			0.0130± 0.0031	1.3150± 0.4077	0.9867± 0.0049	6.9349± 0.0347	0.0003± 0.00003	60.9158 ±0.3046	6.8802± 0.0487	7.9255

Table S2: Amplitudes (A^{cor}) and time constants (τ^{cor}) obtained from the fits of the TCSPC data corrected for the different fractions which were covered by the detection bandpass. Depicted are also the "corrected" amplitude-weighted average lifetimes ($\overline{\tau^{cor}}$) and the increase of the "corrected" averaged lifetime ($\overline{\tau_{rel}^{cor}}$) compared to the lifetime of NMA in absence of SCat.

[SCat] / 10^{-4} M	A_1^{cor}	τ_1 / ns	A_2^{cor}	τ_2 / ns	A_3^{cor}	τ_3 / ns	A_4^{cor}	τ_4 / ns	$\overline{\tau^{cor}}$ / ns	$\overline{\tau_{rel}^{cor}}$
0	0.5959	0.7134	0.4040	1.0922			0.0001	18.2915	0.8686	1.0000
1.84	0.3228	0.6920	0.2675	1.1030	0.4096	6.8600	0.00007	60.7553	3.3327	3.8390
3.69	0.3275	0.7510	0.0920	1.3540	0.5805	6.8700	0.00006	59.8018	4.3619	5.0245
5.53	0.2469	0.7340	0.0799	1.3470	0.6731	6.8700	0.00011	57.4952	4.9192	5.6665
6.33	0.2236	0.7440	0.0678	1.3640	0.7086	6.8800	0.00010	62.2727	5.1400	5.9209
7.38	0.2208	0.7590	0.0470	1.5300	0.7321	6.8800	0.00010	58.0402	5.2819	6.0844
22.1	0.1074	0.7919	0.0144	2.9060	0.8781	6.9130	0.00010	59.7150	6.2027	7.1450

Spectrally Resolved TCSPC Measurement of NMA in Solution

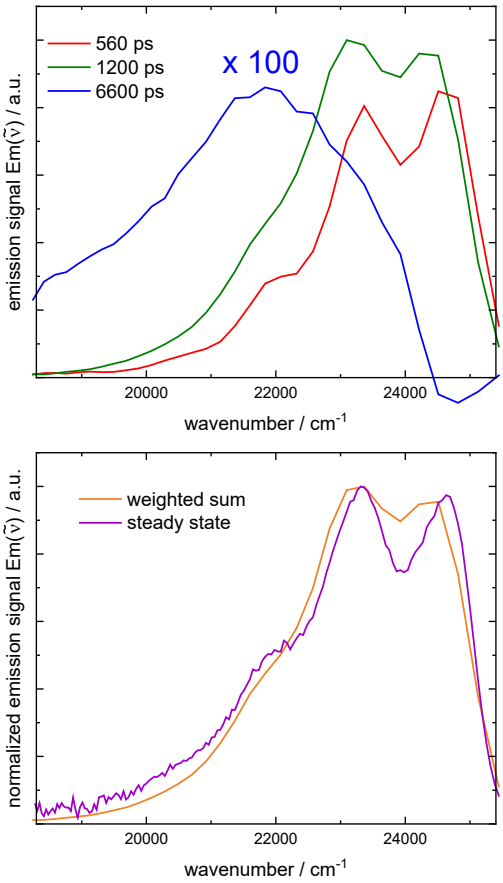

Figure S5: Emission spectrum of NMA in toluene. Top panel: Decay associated spectra (DAS, red, green and blue (scaled by a factor of 100)) obtained from a global fit of the TRES measurement. Bottom panel: Steady state spectrum (purple) and the weighted sum (orange) of the DAS.

^{1}H NMR Measurment of NMA, SCat and the Mixture in Solution

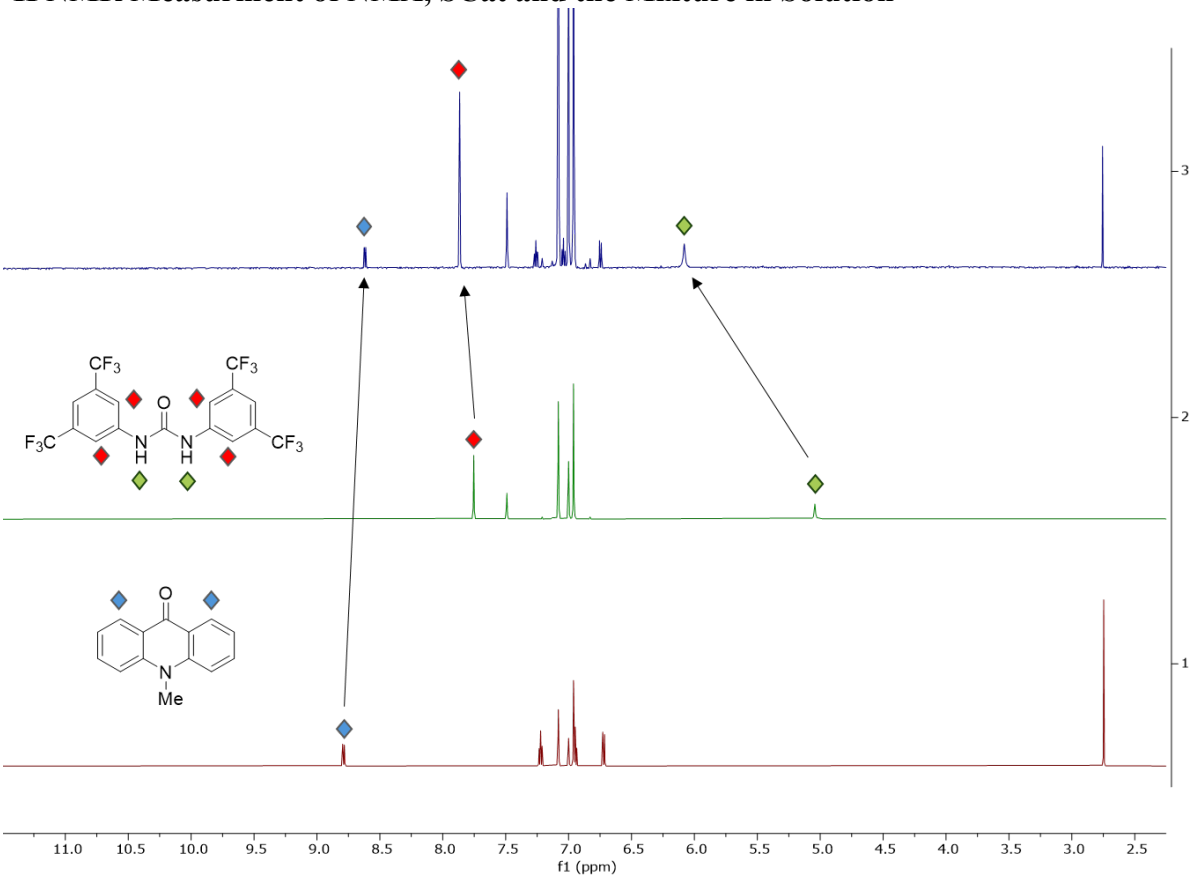

Figure S6: ^{1}H NMR spectra of 10-methylacridin-9(10*H*)-one, 1,3-bis(3,5-bis(trifluoromethyl)phenyl)urea and a mixture of both (concentrations always 0.1 M in toluene-d_8); in the mixture of both a ratio of ca. 1 to 3:1 acridone to urea was present; the aromatic protons in 1,8-position of the acridone are marked with blue diamonds and the aromatic protons of the 1,3-bis(3,5-bis(trifluoromethyl)phenyl)urea are marked with red diamonds, the respective urea protons are marked with green diamonds.

Crystallographic details

Table S3: Crystallographic data of NMA···SCat co-crystal and SCat single crystals.

	NMA···SCat	**SCat**
Empirical formula	$C_{17}H_8F_{12}N_2O$, $C_{14}H_{11}NO$	$C_{17}H_8F_{12}N_2O$
Formula weight	693.49	484.25
Temperature /K	149.99(10)	150.00(10)
Crystal system	triclinic	triclinic
Space group	$P\bar{1}$ (no. 2)	$P\bar{1}$ (no. 2)
***a* / Å**	8.4376(2)	9.0838(2)
***b* / Å**	13.4590(3)	12.8101(3)
***c* / Å**	14.4668(3)	16.3601(3)
***α* / °**	115.684(2)	77.989(2)
***β* / °**	96.017(2)	84.130(2)
***γ* / °**	103.868(2)	77.399(2)
***V* / Å^3**	1395.90(6)	1813.98(7)
Z	2	4
ρ_{calc} / g/cm^3	1.650	1.773
μ /mm^{-1}	1.419	1.799
***F*(000)**	700.0	960.0
Crystal size /mm^3	0.23 × 0.09 × 0.04	0.11 × 0.06 × 0.03
Radiation	Cu Kα (λ = 1.54184)	Cu Kα (λ = 1.54184)
2θ range for data collection / °	6.982 to 152.848	5.532 to 159.314
Index ranges	$-9 \le h \le 10$, $-16 \le k \le 16$, $-17 \le l \le 18$	$-11 \le h \le 11$, $-16 \le k \le 16$, $-20 \le l \le 20$
Reflections collected	35566	68318
Independent reflections	5637 [R_{int} = 0.0664, R_{sigma} = 0.0349]	7734 [R_{int} = 0.0958, R_{sigma} = 0.0475]
Data/restraints/parameters	5637/9/593	7734/174/677
Goodness-of-fit on F^2	1.052	1.030
T_{min} / T_{max}	0.599, 1.000	0.804, 1.000
Final R indexes [$I \ge 2\sigma(I)$]	R_1 = 0.0378, wR_2 = 0.1004	R_1 = 0.0636, wR_2 = 0.1204
Final R indexes [all data]	R_1 = 0.0449, wR_2 = 0.1048	R_1 = 0.0817, wR_2 = 0.1279
Largest diff. peak/hole / e Å^{-3}	0.22/-0.25	0.45/-0.43

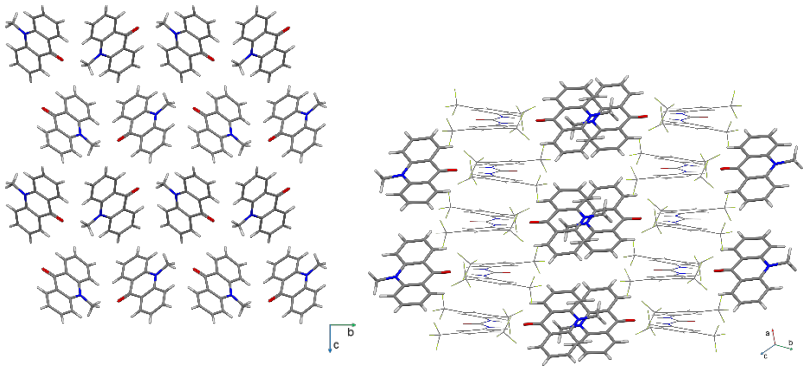

Figure S7: Packing of NMA (left) and NMA···SCat co-crystal (right). The Figure on the left displays the herringbone pattern of stacked NMA units propagating in columns along the *a* axis. (Right) Rearranged slipped stacking sandwiches of NMA are separated by SCat columns formed *via* strong hydrogen bonds between each NMA and SCat entity. SCat is displayed in wireframe style for clarity.

The X-ray powder diffraction (XRPD) pattern of the NMA···SCat co-crystals at room temperature and the Rietveld refinement based on the single-crystal structure measured at 150 K is depicted in Fig. S8. No additional Bragg reflections could be identified that would indicate the presence of a secondary phase.

Table S4: Derived lattice parameters from the Rietveld refinement of the powder diffraction pattern measured at ambient conditions.

Crystal system	triclinic
Space group	$P\bar{1}$ (no. 2)
Z	2
Radiation, λ / Å	Cu $K_{\alpha 1}$, 1.5406
***a* / Å**	8.583(3)
***b* / Å**	13.66(4)
***c* / Å**	14.70(4)
***α* / °**	114.717(8)
***β* / °**	97.08(2)
***γ* / °**	105.08(2)
***V* / Å^3**	1457.75
2*θ* range / °	5.0 – 70.0
2*θ* step width / °	0.008
R_{exp}, %	0.845
R_{wp}, %	8.902
R_{p}, %	6.660
R_{Bragg}, %	1.987
G.o.o.F.	10.531

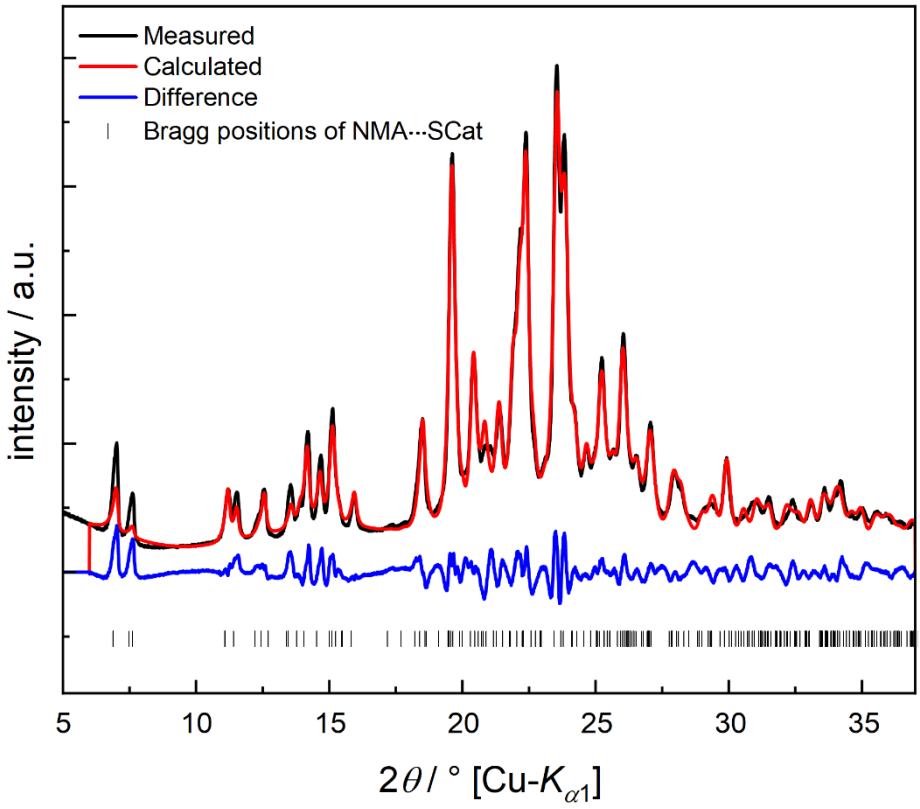

169

170 **Figure S8**: Experimental X-ray powder diffraction pattern of NMA···SCat (black) at 298 K
171 compared to its theoretical pattern (red) simulated from single-crystal data obtained at 150 K
172 (see Table S4).

173

174 **Experimental and SCXRD Details of SCat Crystal Structure**

175 SCat single crystals were obtained from dissolution of 2 mg (4,13 µmol) SCat in 2 mL toluene
176 and slow evaporation of the solvent at ambient temperature. The asymmetric unit consists of
177 two SCat molecules arranged twisted at a 53° angle. The bifurcated N–H···O interactions
178 (N3A–H···O1A 2.809(2) Å, N4A–H···O1A 2.807(2) Å, and N2A–H···O2A 2.845(2) Å, N1A–
179 H···O2A 2.838(2) Å) between the carboxylic and the urea group form hydrogen bonded chains
180 along the crystallographic *a* axis throughout the crystal structure. Aromatic rings of SCat units

are connected via $\pi\cdots\pi$ stacking interactions with centroid-centroid distances of 3.6535(14) Å and 3.7330(13) Å, respectively.

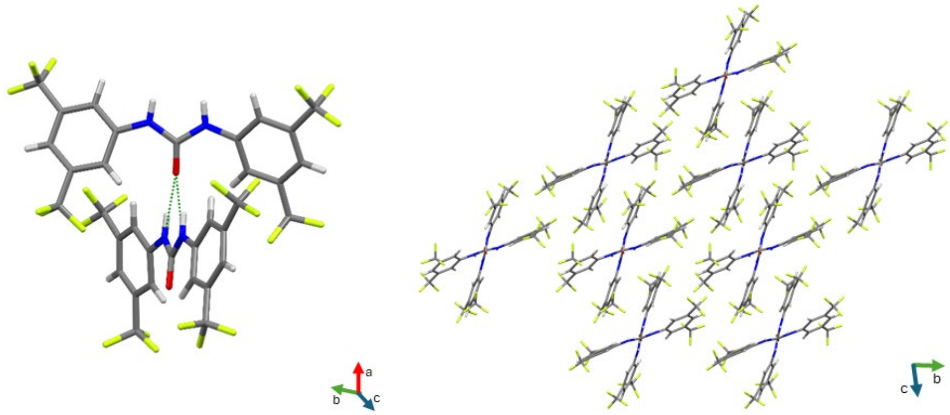

Figure S9: Crystal structure of SCat with Z´= 2. Bifurcated N–H···O interactions connect the carboxylic and the urea group. One SCat molecule in the asymmetric unit is involved in π-stacking interactions forming chains along the crystallographic *b* axis. The crystal packing (right) is displayed in a view along the crystallographic *a* axis.

IR Spectra of NMA, SCat and NMA···SCat in the Solid State

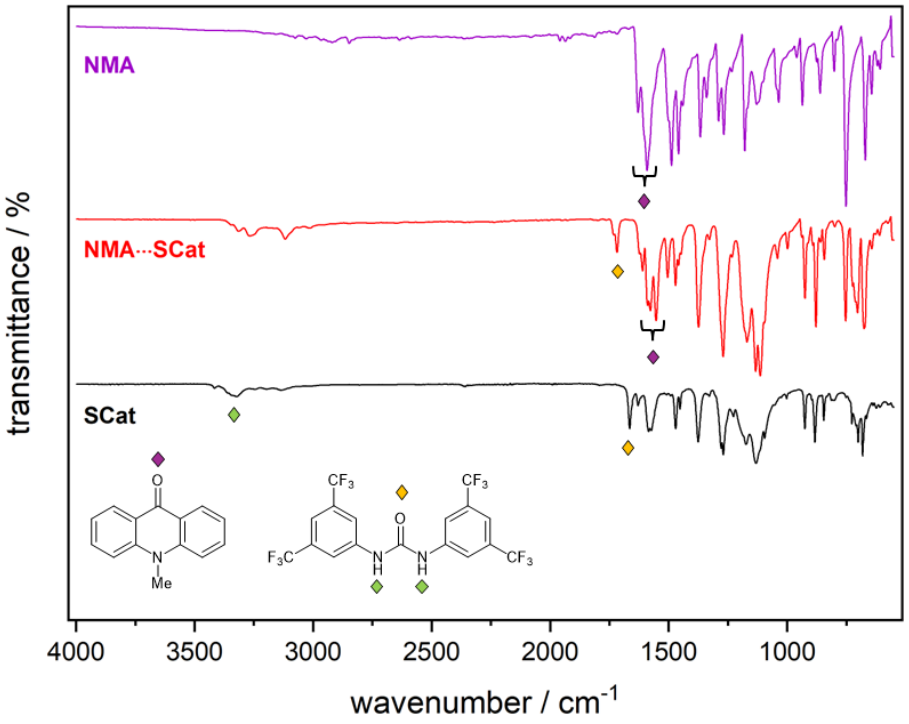

Figure S10: FTIR spectra of the NMA, NMA···SCat co-crystal and SCat measured at ambient temperature in the range of 4000 cm^{-1} to 550 cm^{-1}.

Emission and Excitation Spectroscopy of NMA and NMA···SCat in the Solid State

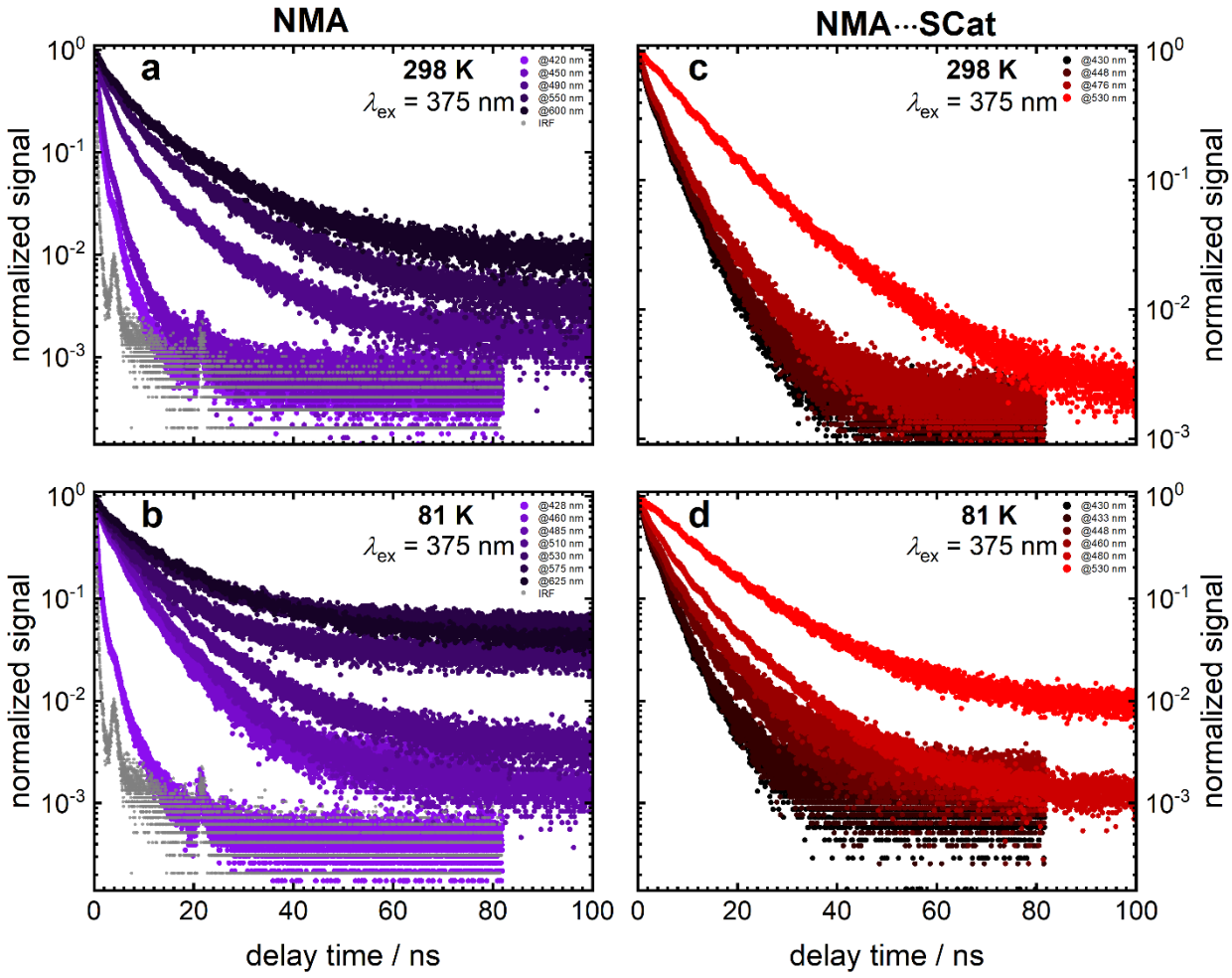

Figure S11: Luminescence decay measurements of NMA and NMA···SCat detected at different emission wavelengths under direct excitation at 298 K (a, c) and 81 K (b, d). The resulting decay times are compiled in Table S5 and S6.

Table S5: Amplitudes and lifetimes of NMA under direct excitation, detected at different emission wavelengths at 298 K. The corresponding luminescence decay measurements are depicted in Figure S11a.

λ_{em} / nm	A_1	τ_1 / ns	A_2	τ_2 / ns	A_3	τ_3 / ns
420	0.848±0.008	0.486±0.015	0.15±0.005	1.988±0.04	0.002±0.001	9.479±1.422
450	0.759±0.008	0.666±0.027	0.235±0.019	2.246±0.067	0.006±0.002	8.723±0.959
490	0.207±0.002	0.550±0.007	0.657±0.002	2.84±0.013	0.126±0.002	10.638±0.077
550	0.472±0.010	2.053±0.029	0.448±0.006	6.336±0.156	0.106±0.007	18.039±0.516
600	0.295±0.0172	2.270±0.079	0.532±0.011	6.506±0.204	0.17±0.01	18.759±0.465

Table S6: Amplitudes and lifetimes of NMA under direct excitation, detected at different emission wavelengths at 81 K. The corresponding luminescence decay measurements are depicted in Figure S11b.

λ_{em}/ nm	A_1	τ_1 / ns	A_2	τ_2 / ns	A_3	τ_3 / ns
428	0.777±0.007	0.639±0.032	0.216±0.015	2.327±0.093	0.006±0.002	8.797±1.32
460	0.381±0.006	1.457±0.017	0.632±0.004	5.012±0.065	0.038±0.007	12.856±0.874
485	0.275±0.007	1.545±0.028	0.656±0.005	4.969±0.069	0.081±0.008	12.776±0.429
510	0.298±0.009	1.73±0.038	0.617±0.006	5.642±0.103	0.119±0.009	15.188±0.426
530	0.274±0.013	1.638±0.064	0.583±0.009	6.093±0.188	0.128±0.014	16.97±0.778
575	0.235±0.011	1.778±0.085	0.536±0.009	7.302±0.237	0.161±0.013	21.781±0.823
625	0.259±0.008	2.656±0.086	0.593±0.006	10.622±0.19	0.086±0.006	36.945±1.274

Table S7: Amplitudes and lifetimes of NMA···SCat under direct excitation, detected at different emission wavelengths at 298 K. The corresponding luminescence decay measurements are depicted in Figure S11c.

λ_{em}/ nm	A_1	τ_1 / ns	A_2	τ_2 / ns	A_3	τ_3 / ns
430	0.330±0.006	1.241±0.018	0.659±0.004	4.467±0.059	0.022±0.007	12.625±1.817
448	0.229±0.007	1.240±0.023	0.689±0.006	4.622±0.07	0.03±0.01	12.056±1.646
476	0.273±0.009	1.431±0.033	0.681±0.009	5.052±0.103	0.064±0.015	12.433±1.088
530	0.973±0.005	9.580±0.035	0.054±0.005	26.014±1.25		

Table S8: Amplitudes and lifetimes of NMA···SCat under direct excitation, detected at different emission wavelengths at 81 K. The corresponding luminescence decay measurements are depicted in Figure S11d.

λ_{em}/ nm	A_1	τ_1 / ns	A_2	τ_2 / ns	A_3	τ_3 / ns
430	0.459±0.004	1.293±0.01	0.558±0.004	3.958±0.015		
433	0.427±0.004	1.254±0.009	0.580±0.004	4.02±0.014		
448	0.443±0.008	1.407±0.018	0.560±0.005	4.562±0.076	0.026±0.006	14.335±1.713
460	0.449±0.007	1.236±0.02	0.609±0.005	4.574±0.075	0.072±0.009	12.399±0.664
480	0.322±0.005	1.438±0.024	0.627±0.006	5.281±0.07	0.158±0.009	12.277±0.237
530	0.954±0.002	10.333±0.029	0.0296±0.003	42.131±3.161		

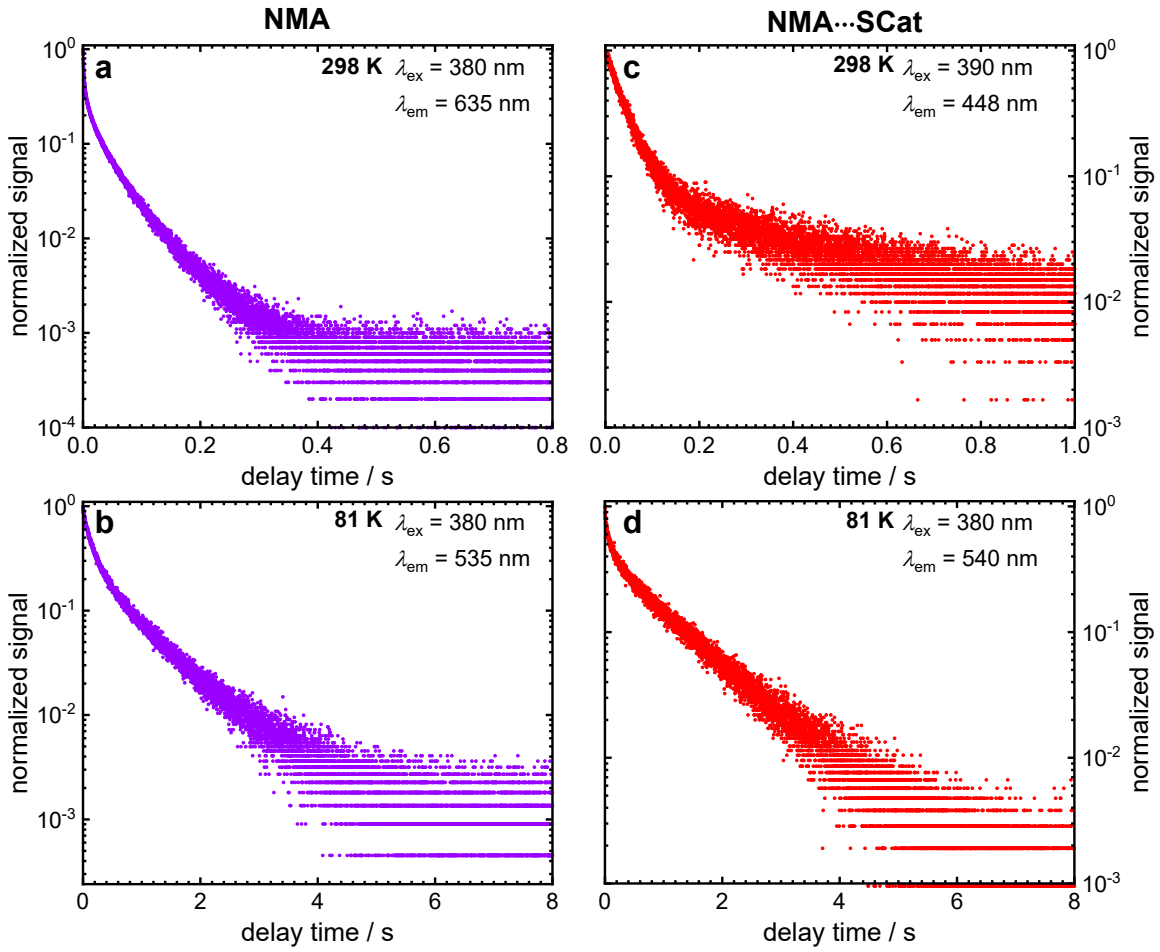

Figure S12: Luminescence decay measurements of NMA and NMA···SCat from 1 ms onwards at 298 K (a, c) and 81 K (b, d). The detected emission wavelength corresponds with the emission maximum after a 1 ms delay. The resulting decay times are depicted in Table S9 and S10.

Table S9: Amplitudes and lifetimes of NMA and NMA···SCat after a 1 ms delay at 298 K. The corresponding luminescence decay measurements are depicted in Figure S12 (a, c).

	A_1	τ_1 / ms	A_2	τ_2 / ms	A_3	τ_3 / ms
NMA	0.537±0.001	1.206±0.005	0.259±0.001	8.987±0.059	0.188±0.001	46.357±0.127
MPK002	0.893±0.002	35.8403±0.145	0.08224±0.002	287.897±9.044		

Table S10: Amplitudes and lifetimes of NMA and NMA···SCat after a 1 ms delay at 81 K. The corresponding luminescence decay measurements are depicted in Figure S12 (b, d).

	A_1	τ_1 / ms	A_2	τ_2 / ms	A_3	τ_3 / ms
NMA	0.152±0.003	21.66±0.746	0.545±0.002	148.274±1.125	0.281±0.002	757.495±3.463
MPK002	0.427±0.002	75.619±0.701	0.417±0.001	948.542±3.023		

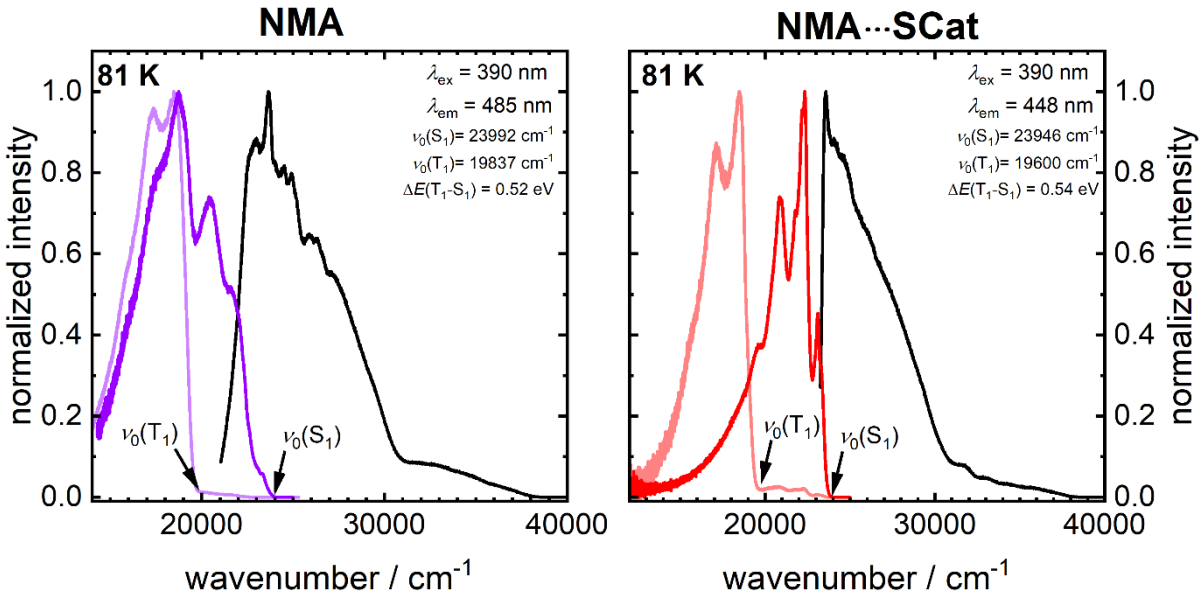

Figure S13: Excitation (black) and emission spectra of NMA (violet) and NMA···SCat (red) at 81 K. The emission after a 1 ms delay is depicted in the corresponding desaturated color. To estimate the energy gap $\Delta E_{S_1T_1}$, the highest onset energy of the fluorescence and phosphorescence band was determined (see markings).

Additional quantum chemical results

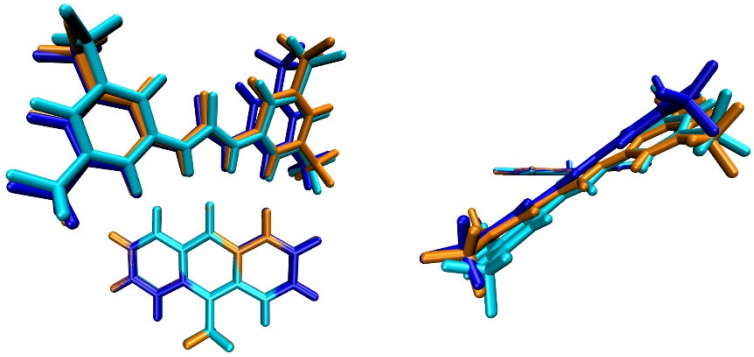

Figure S14: Different perspective on the overlay of optimized geometries in different environments. This overlay shows that the environment (PCM and QM-MM) has only a minute effect on the geometry. Toluene (blue), crystal structure with optimized hydrogen atoms (orange), optimized structure in solid state environment (turquoise).

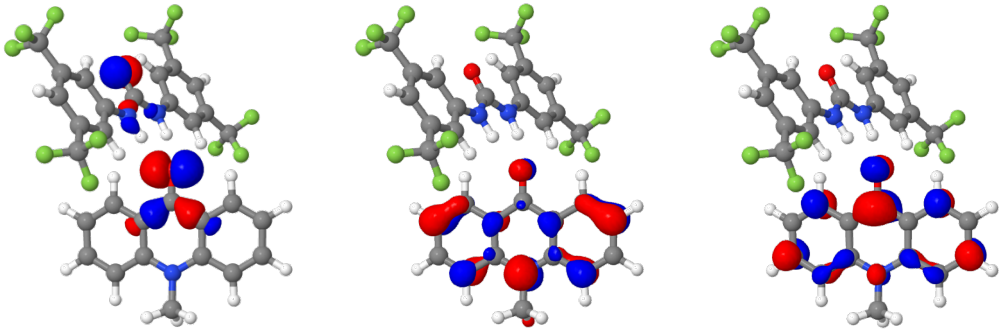

Figure S15: Orbitals that are involved in the relevant energetically lowest transitions at the optimized ground state geometry. From left to right: HOMO-8 (n-orbital), HOMO (π-orbital), LUMO (π-orbital).

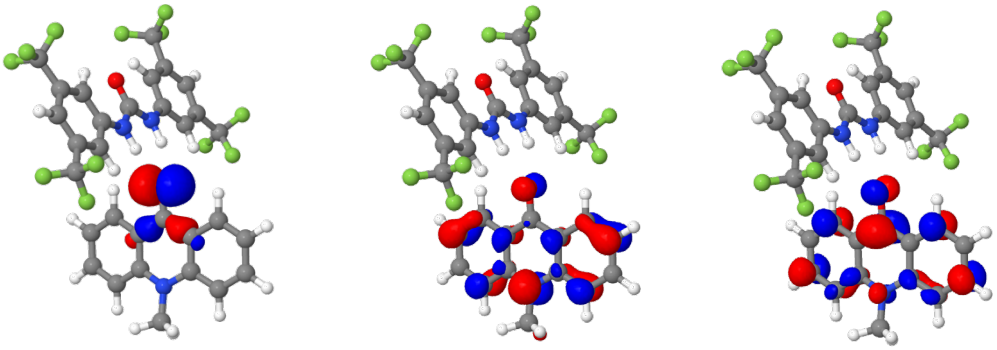

Figure S16: Orbitals that are involved in the energetically lowest transitions at the optimized $n\pi^*$-triplet state geometry. From left to right: HOMO-8 (n-orbital), HOMO (π-orbital), LUMO (π-orbital).

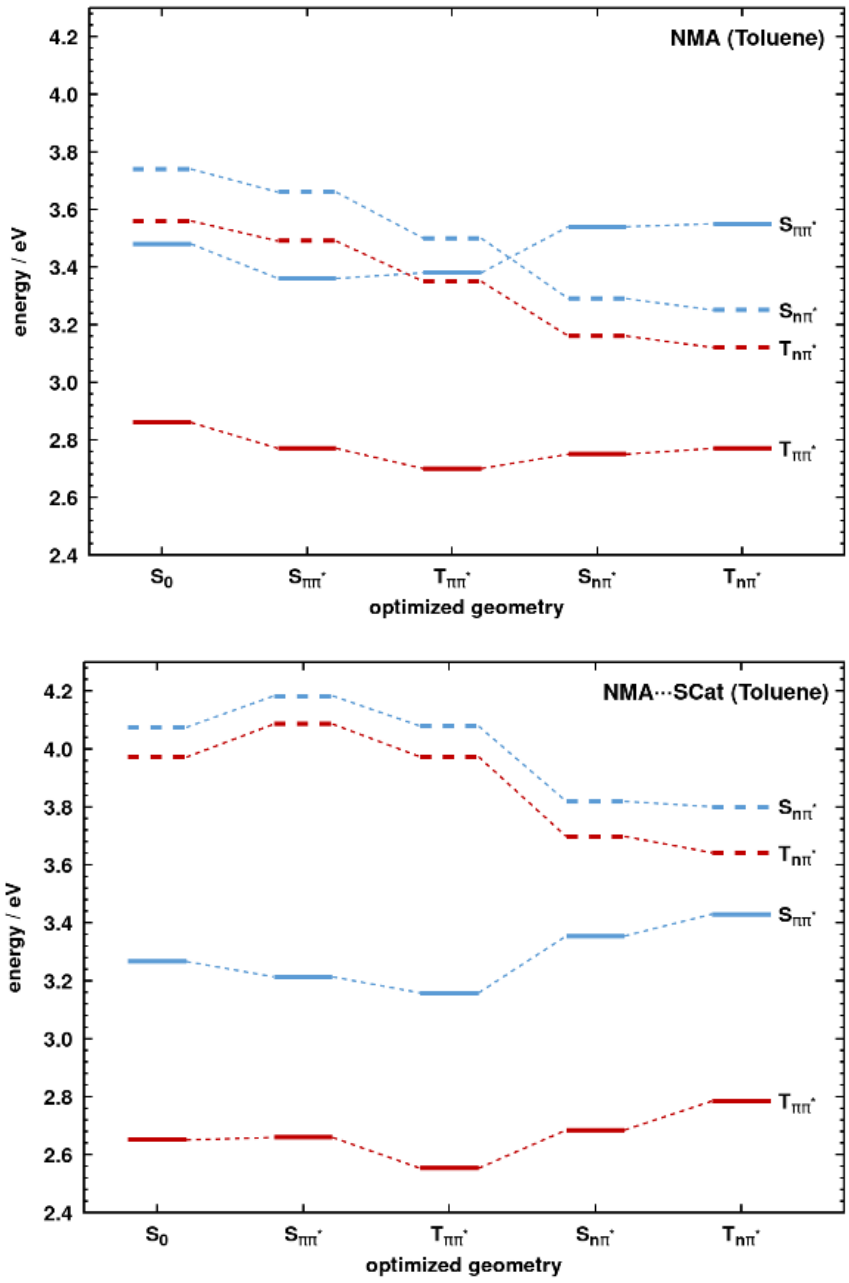

Figure S17: Adiabatic energies without ZPVE correction for the electronic ground state and the optimized geometries of selected lowest excited states of NMA (left) and NMA···SCat (right). In both cases, the $^1n\pi^*$ represents the S_2 state at the ground-state geometry. The $^3n\pi^*$ state is found as the tenth excited triplet state (T_{10}) in the NMA···SCat complex. Intermediate $^3\pi\pi^*$ states lying energetically about 0.9 – 1 eV above the T_1 ($^3\pi\pi^*$) state have been omitted.

Thermogravimetric analysis

The TG data show a complete one-step degradation for each of the starting materials and the co-crystal. Additionally, NMA and NMA···SCat exhibit partial sublimation prior to the onset of thermal decomposition. This effect is more pronounced in the pure NMA which repeatedly causes spikes in the respective curve.

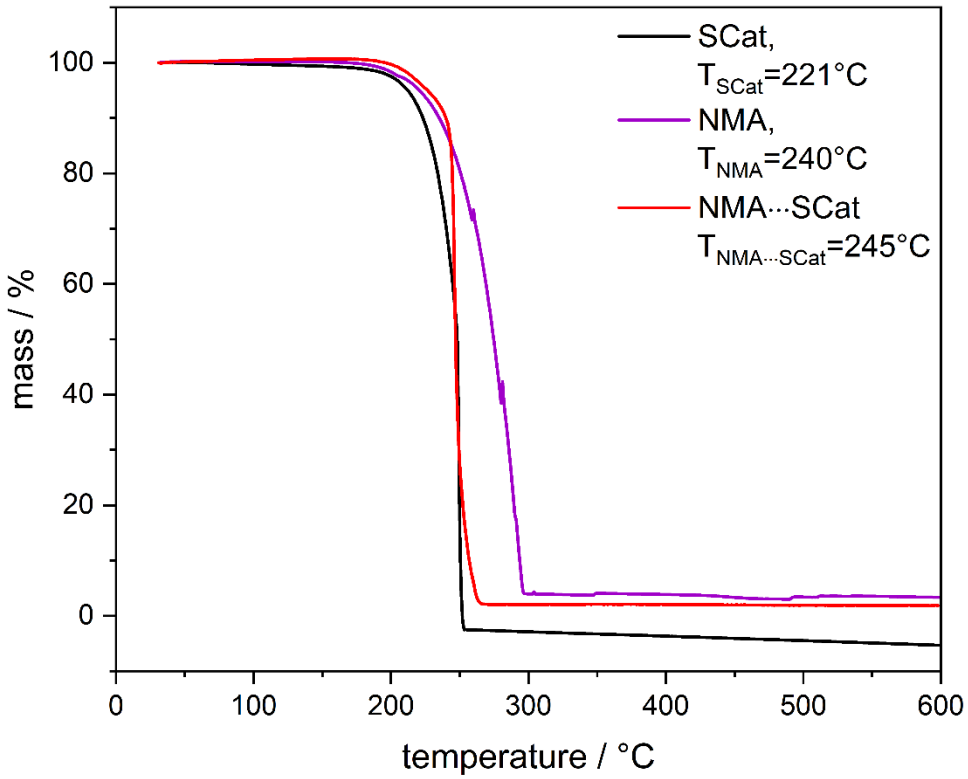

280

281 **Figure S18**: TG curves of NMA, SCat and NMA···SCat with onset decomposition
282 temperatures, measured under the synthetic air/nitrogen atmosphere from 30 °C to 600 °C. The
283 mass loss amounts 96% for NMA, 100% for SCat and 98% for NMA···SCat.

REFERENCES

1. K. Hirose, *J. Incl. Phenom. Macrocycl. Chem.*, 2001, **39**, 193-209.
2. P. Thordarson, *Chem. Soc. Rev.*, 2011, **40**, 1305-1323.
3. S. W. Benson, *The Foundation of Chemical Kinetics*, McGraw Hill Book Company Inc, New York, 1960.
4. M.-C. Justice and J.-C. Justice, *J. Solution Chem.*, 1976, **5**, 543-561.
5. J. B. Maglic and R. Lavendomme, *J. Appl. Cryst.*, 2022, **55**, 1033-1044.
6. O. Peterson, J. Webb, W. McColgin and J. Eberly, *J. Appl. Phys.*, 1971, **42**, 1917-1928.
7. A. Deshpande, A. Beidoun, A. Penzkofer and G. Wagenblast, *Chem. Phys.*, 1990, **142**, 123-131.
8. T. Villnow, G. Ryseck, V. Rai-Constapel, C. Marian and P. Gilch, *J. Phys. Chem. A.*, 2014, **118**, 11696-11707.